Highly Asymmetric Interactions between Globin Chains during Hemoglobin Assembly Revealed by Electrospray Ionization Mass Spectrometry†

Wendell P. Griffith and Igor A. Kaltashov*

Department of Chemistry, University of Massachusetts, Amherst, Massachusetts 01003

Received January 9, 2003; Revised Manuscript Received June 30, 2003

ABSTRACT: Dynamics of bovine hemoglobin assembly was investigated by monitoring monomers/oligomers equilibria in solution with electrospray ionization mass spectrometry and circular dichroism spectroscopy. Intensities of ionic signals corresponding to various protein species (tetramers, dimers, heme-deficient dimers, as well as apo- and holo-monomers) were used to estimate relative fractions of these species in solution as a function of pH. The fraction of folded protein for each observed species was estimated based on charge-state distributions of corresponding ionic species in the mass spectra. The cumulative numbers (averaged across the entire protein population) were in good agreement with circular dichroism data at the Soret band and in the far-UV region, respectively. The mass spectral data confirm that hemoglobin dissociation involves a step where heme is first lost from the β-chain of the $\alpha\beta$-dimer to form a heme-deficient dimeric species. This dimer dissociates further to produce a holo-α-chain and an apo-β-chain. The former is tightly folded into a comparatively compact structure at neutral pH, while the latter always exhibits significant backbone disorder. Acidification of the protein solution to pH 4 leads to partial heme dissociation and significant increase of the backbone flexibility in the α-chains as well. Complete dissociation of the heme from the α-chains at a pH below 4 coincides with the total disappearance of the dimeric and tetrameric hemoglobin species from the mass spectra. The experimental data provide strong evidence that binding of a partially unstructured apo-β-chain to a tightly folded holo-α-chain to form a heme-deficient dimer is the initial step of hemoglobin assembly. Such binding locks the β-chain in a highly ordered conformation, which allows for an efficient heme acquisition, followed by docking of two hemoglobin dimers to form a tetrameric form of the protein. The asymmetry of the roles of the two chains in the assembly process is surprising, given a rather high sequence homology (ca. 43%) and highlights functional importance of intrinsic protein disorder. The study also demonstrates a tremendous potential of mass spectrometry as an analytical tool capable of elucidating protein interaction mechanisms in highly heterogeneous systems.

Mammalian hemoglobins (Hb)[1] are among the most studied proteins and have long served as a paradigm for cooperativity and allostery (*1*, *2*). Hence, the majority of the research efforts have been geared toward the characterization of ligand-binding properties of this protein, whose major function is the physiological transport of oxygen in the blood. Recently, there has been renewed interest in understanding the dynamics of Hb assembly and dissociation. Several factors stimulated this interest. First, the dissociation behavior of the Hb molecule has a direct effect on its oxygen-binding properties. Second, several disorders have been linked to abnormalities in the Hb association process (*3*, *4*). Last, since Hb scavengers such as haptoglobin do not bind to the intact protein, Hb dissociation is an important determinant of its rapid clearing from circulation during hemolysis (*5*) or following the transfusion of Hb based oxygen carriers (*6*).

Most mammalian Hb molecules have a tetrameric structure with a molecular mass of approximately 64.5 kDa (*7*). They are composed of two pairs of α- and β-subunits containing 141 and 146 amino acid residues, respectively. The four subunits have the same tertiary fold, with the α- and the β-chains containing seven and eight α-helices, respectively (*7*). Structures of the oxygen-bound and oxygen-free forms of Hb reveal significant differences (*7*−*9*), thus allowing the dynamics of the ligand-binding process to be deduced based largely on such static snapshots. Contrary to that, studies of the Hb assembly/dissociation processes have to rely on spectroscopic methods that provide both structural and dynamic information. Another intrinsic difficulty is a highly heterogeneous character of the Hb system. Once released from a red blood cell, Hb tetramers can dissociate to heterodimers and in dilute solutions further to globin monomers (*10*). All stages of interactions between subunits in the assembly process and the reciprocal dissociation process are in continuous and rapid equilibrium (*11*). The tetramer−dimer equilibrium constant is on the order of 2 μM for liganded Hb, which has a higher tendency to dissociate than the deoxy tetramers (*12*, *13*). An equilibrium also exists between the protein globin and the hemin

† Supported in part by a grant from the National Institutes of Health R01 GM61666.

* To whom correspondence should be addressed. Phone: (413) 545-1460. Fax: (413) 545-4490. E-mail: kaltashov@chem.umass.edu.

[1] Abbreviations: Hb, hemoglobin; ESI MS, electrospray ionization mass spectrometry; CD, circular dichroism; UV, ultraviolet; *m*/*z*, mass-to-charge ratio.

10.1021/bi034035y CCC: $25.00
Published on Web 07/31/2003

prosthetic group (*14*). The Hb equilibrium processes are affected by a number of extrinsic factors. These include pH, denaturing agents, temperature, and organophosphates (*15*).

Some of the physicochemical methods used to study the Hb tetramer−dimer equilibrium are chromatography, sedimentation, light scattering, auto-oxidation, and the binding of Hb to haptoglobin (*15*). However, there are no quick, easy, and reliable methods for making species-specific measurements in Hb solutions because of its highly heterogeneous character (Hb dimers have spectral and ligand-binding properties very similar to those of the fully liganded tetramer) (*15*).

As a result of extensive research efforts in the past decade, a picture of Hb assembly/dissociation is now beginning to emerge (*16*). It has been proposed that there may be three distinct pathways of Hb tetramer assembly: through a heme-containing heterodimer ($\alpha^*\beta^*$), a semihemoglobin ($\alpha\beta^*$ or $\alpha^*\beta$), or an apo-Hb dimer ($\alpha\beta$) (*17*). Recently, in vitro evidence has been provided for the pathway that includes an $\alpha^*\beta$-intermediate that ensures correct formation of the active Hb tetramers (*16*), which may be also important for understanding the in vivo Hb assembly pathway. Some of these intermediates may also have physiological significance as species designed for facile recognition by haptoglobin and heme scavengers outside the erythrocytes following hemolysis (*14*).

Over the past several years, an explosive growth of electrospray ionization (ESI) mass spectrometry (MS) has enabled the study of numerous noncovalent protein complexes (*18*−*20*). Following the pioneering work by Chowdhury et al. (*21*) and Loo et al. (*22*), it has been also used as a qualitative probe of protein conformational changes in solution. It is now becoming an increasingly popular technique to probe protein higher order structure and dynamics under a variety of conditions (*23*). ESI MS has also played a prominent role in hemoglobin research; however, its applications have been mostly limited to sequence analysis of various Hb forms, variants, and mutants (*24*); posttranslational modification of Hb (*25*); and quaternary structure of giant extracellular Hb molecules from nonvertebrate organisms (*26*, *27*).

In the present work, we are using ESI MS as a tool to monitor Hb assembly/dissociation equilibria as a function of solution pH. The experimental data provide strong support to the notion that a Hb tetramer assembly proceeds through a heme-deficient dimer (αheme-βglobin, or $\alpha^*\beta$) intermediate. The latter is formed via association of a tightly folded holo form of the α-chain (α^*) and a highly unstructured apo-form of the β-chain (β). Flexibility of the β-chain appears to be an important factor facilitating the $\alpha^*\beta$-dimer formation by allowing easy adoption of the native-like structure by the β-chain on a rigid template (α^*). Formation of the $\alpha^*\beta$-dimer locks the β-chain conformation in a highly structured native or native-like conformation, which allows for a robust heme acquisition, leading to the formation of an $\alpha^*\beta^*$-dimer and eventually to a $(\alpha^*\beta^*)_2$-tetramer.

EXPERIMENTAL PROCEDURES

Materials. Bovine Hb and horse heart myoglobin (lyophilized powder) were purchased from Sigma Chemical Co. (St. Louis, MO). All sample solutions were prepared from a 1 mM stock solution of Hb in water. All other chemicals, buffers, and solvents were of analytical grade or higher.

Mass Spectrometry. All mass spectra were acquired on a JMS-700 MStation (JEOL, Tokyo, Japan) two-sector mass spectrometer equipped with a standard ESI source. The Hb sample solutions were prepared by diluting the stock solution in 10 mM ammonium acetate solution whose pH (in the range 3−10) was adjusted to a desired level with NH_4OH or CH_3CO_2H. The final protein concentration in each sample was 10 μM. All solutions were equilibrated at room temperature (24 °C) for 1 h prior to analysis. The appearance of spectra did not change for any of the longer equilibration times investigated. The samples were introduced into the ESI source at flow rates of 3 μL/min. All ESI source settings (temperature in the desolvation region, electrostatic potentials on all ion-optical elements, and settings of the quadrupole ion guide) were chosen to minimize the gas-phase decomposition of the Hb noncovalent complexes at physiological pH. To investigate the effect of the ESI source settings on the gas-phase dissociation of the Hb ions and to choose the optimal parameters (i.e., those settings that minimize dissociation), a series of Hb spectra was acquired at neutral pH (Supporting Information). The optimal source parameters were determined by increasing the source temperature and skimmer potential in a stepwise fashion from their lowest values to achieve adequate protein ion desolvation and a signal-to-noise ratio with no change in the appearance of the distributions of the species in the mass spectrum (vide infra). The optimal source settings were found to be as follows: orifice potential, 0 V; ring lens potential, 55 V; orifice temperature, 120 °C; and desolvating plate temperature, 80 °C. These ESI source settings were kept constant throughout all measurements to avoid any possible changes in the ion desorption and transmission conditions. The spectra were acquired by scanning the magnet at a rate of 5 s/decade. To ensure a high signal-to-noise ratio, 500 scans were averaged to record each spectrum. ESI spectra were processed (peak integration) using Microcal Origin (Microcal Software, Inc., Northampton, MA) software.

Circular Dichroism. All CD experiments were performed with a JASCO J-715 CD spectropolarimeter (Jasco Corporation, Tokyo, Japan) at 20 °C. Sample preparation was exactly the same as for the mass spectrometry section. Spectra for two regions were recorded: the far-UV region (200−250 nm) and the near-UV/vis region (250−600 nm). A 1 mm path length was used for both sets of experiments. For the far-UV CD, the following instrumental settings were used: step resolution, 1 nm; scan speed, 50 nm/min; response, 2 s; bandwidth, 1 nm; sensitivity, 50 mdeg; and slit width, 1000 μm. For the near-UV CD, similar instrumental settings were used with the following differences: sensitivity, 20 mdeg and scan speed, 100 nm/min. In each region, spectra were recorded as an average of five scans.

RESULTS

Mass Spectrometry. Figure 1 shows a typical mass spectrum of bovine Hb at near-physiological pH (pH 8). Under these conditions, protein ion peaks appear to be wide because of incomplete desolvation in the gas phase. Mass assignment for such peaks has been done using a procedure introduced by Amster et al. (*28*). In brief, acquisition of a

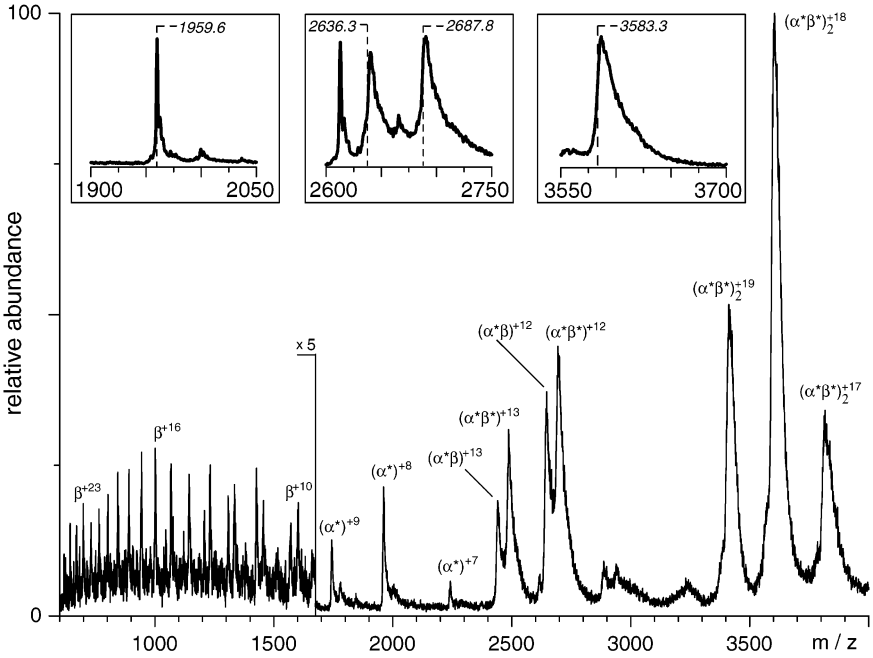

FIGURE 1: ESI mass spectrum of a 10 μM bovine Hb solution in 10 mM ammonium acetate pH 8. Presence of a heme group on globin chains is indicated with (*). Ionic signal below *m*/*z* 1675 has been multiplied by a factor of 5 for clear visualization. On the insets (from left to right) peak shapes of $(\alpha^*)^{+8}$, $(\alpha^*\beta^*)^{+12}$, $(\alpha^*\beta)^{+12}$, and $(\alpha^*\beta^*)_2^{+18}$ ions in the mass spectrum acquired under conditions favored better desolvation and partial dissociation of the noncovalent protein complex ions in the gas phase (full spectra are presented in Supporting Information). Calculated masses are marked with dotted lines.

mass spectrum under mild ESI conditions was followed by an increase of the orifice potential (cone voltage) and/or desolvating temperature. Although these harsher conditions resulted in partial dissociation of noncovalent protein complexes (vide infra), the desolvation of the surviving complex ions was significantly improved. This allowed the survivor ion peaks to be assigned with high confidence (see insets in Figure 1).

Multiple species are present in the spectrum, corresponding to monomers, dimers, and a tetramer, with the latter one being the most abundant in the spectrum. In addition to the abundant ionic signal corresponding to the Hb dimer ($\alpha^*\beta^*$), the mass spectrum also shows the existence of a dimeric species lacking one heme (labeled $\alpha^*\beta$ in Figure 1). This species has previously been suggested to be an obligatory intermediate in the Hb association/dissociation pathway (*16*). No ionic signal corresponding to either a putative apo-dimeric form of Hb ($\alpha\beta$) or homodimers (α_2, α^*_2, β_2, β^*_2) can be detected in the spectrum.

Consistent with earlier reports by Heck and Versluis (*29*) and Loo et al. (*30*), the presence of monomeric globins was detected even at neutral pH. The absence of such ionic species from the ESI spectra of Hb is usually a result of either chemical cross-linking (*31*) or discrimination against low *m*/*z* ions in the mass analyzer (*32*). Importantly, available solution equilibrium data on Hb dissociation (*33*) suggest that monomeric globin chains should be present in solution under conditions used in our experiments. Out of four possible monomeric species (α^*, α, β^*, and β), only the holo-α- and apo-β-chains are present in the spectrum, together accounting for less than 15% of the total ionic signal. In addition to lacking the heme groups, β-chains also exhibit a significantly higher charge density and a broader charge-state distribution, as compared to the α^*-ionic species. This is usually a manifestation of a significantly less compact (mostly unfolded) structure, which allows a larger number of charges to be accumulated on a protein molecule during the ESI process (*34*). Absence of α- and β^*-globin species in the spectrum suggests that the observed heme-deficient dimer (vide supra) is indeed a $\alpha^*\beta$-species.

The dynamics of Hb assembly/dissociation was studied by monitoring a set of equilibria in aqueous solutions in the pH range from 3 to 10, as shown in Figure 2. The tetrameric Hb species $(\alpha^*\beta^*)_2$ dominates the spectra acquired in the pH range 7−9 and is most abundant at pH 8. Putative tetrameric species lacking one or more heme group have not been detected in any of the acquired spectra. The dimeric species ($\alpha^*\beta^*$) dominates the spectra at pH 5, 6, and 10 and is always accompanied by a heme-deficient dimer. The monomeric species dominate the spectra at pH 4 and below. The α-chains retain their heme-binding capacity until the pH is lowered to 4. Heme dissociation from the α-chains is complete at pH 3; however, a significant fraction of the α-chains remains highly structured in solution even under these conditions, as evidenced by a bimodal charge-state distribution of the α-ionic species in the mass spectrum (Figure 2, top trace). A very weak ionic signal corresponding to apo-dimeric species (α_2, $\alpha\beta$, and β_2) with no sign of heme-containing dimers can be seen in this spectrum as well.

At pH > 4, the protein is expected to exist mostly in the natively structured state (*35*); however, the β-chain maintains an unfolded structure, as judged by the broad charge-state distributions and higher average charge density as compared to the α-chains. The holo-β-chains (β^*) have not been observed at any pH. To obtain more detailed information on globin monomers conformations, their charge-state distributions have been processed using a chemometric procedure described in detail elsewhere (*36*). Singular value decomposition (SVD) of the charge-state distributions yielded four significant singular values, indicating the presence of

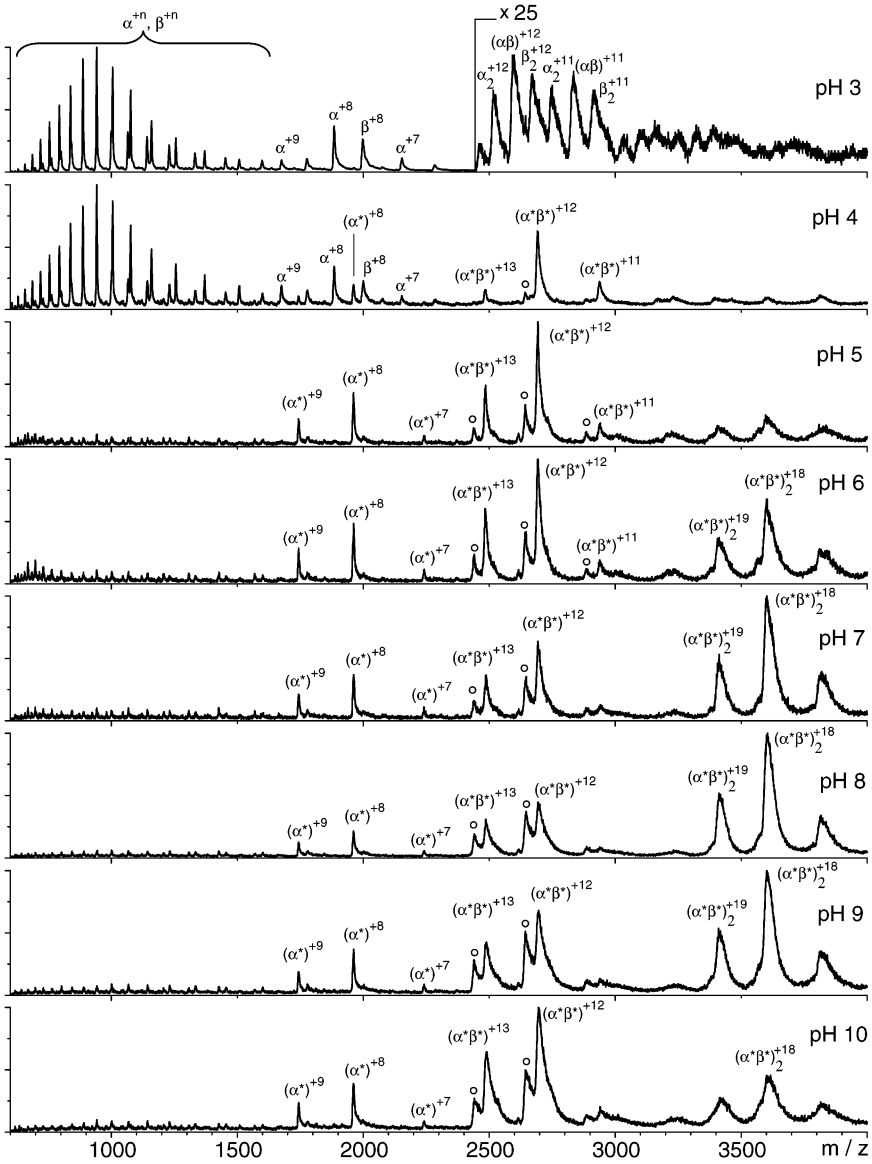

FIGURE 2: ESI mass spectra of 10 μM bovine Hb solutions in 10 mM ammonium acetate arranged in order of increasing pH (from 3 to 10). Ion peaks marked with (○) correspond to the semi-hemoglobin dimers, $\alpha^*\beta$. Ionic signal above *m*/*z* 2400 (in the top spectrum) has been multiplied by a factor of 25 for clear visualization.

four conformers for each globin. Figure 3 presents the results of deconvolution of the charge-state distributions for α*-, α-, and β-globin ions at pH 8 and 4. The assignment of the four detected conformers was done based on the results obtained previously for a structurally similar protein, myoglobin: N, the most compact state; I, an intermediate state (pH 4 intermediate); E, extended conformation; and U, unfolded state (random coil) (*36*). The globin ion signal at charge states +7 through +9 arises mostly because of the contribution from the compact (native or native-like) N state, while the less structured states contribute to the ionic signal at higher charge states (Figure 3). The oligomeric Hb species ($(\alpha^*\beta^*)_2$, $\alpha^*\beta^*$, and $\alpha^*\beta$) always maintain highly structured compact conformations as suggested by low protein charge density and narrow charge-state distributions.

The percentage of natively folded protein and the fraction of heme-bound globin chains have been estimated at each pH by processing the mass spectra in the following fashion. The areas under the mass peaks A_i were used to calculate the following fractions:

$$\%\ \text{compact protein signal} = \frac{4A_{(\alpha^*\beta^*)_2} + 2A_{\alpha^*\beta^*} + 2A_{\alpha^*\beta} + A_{\alpha^*\mathrm{N}} + A_{\alpha\mathrm{N}} + A_{\beta\mathrm{N}}}{4A_{(\alpha^*\beta^*)_2} + 2A_{\alpha^*\beta^*} + 2A_{\alpha^*\beta} + A_{\alpha^*_{\mathrm{total}}} + A_{\beta^*_{\mathrm{total}}} + A_{\alpha_{\mathrm{total}}} + A_{\beta_{\mathrm{total}}}} \times 100 \quad (1)$$

$$\%\ \text{heme-bound protein signal} = \frac{4A_{(\alpha^*\beta^*)_2} + 2A_{\alpha^*\beta^*} + A_{\alpha^*\beta} + A_{\alpha^*}}{4A_{(\alpha^*\beta^*)_2} + 2A_{\alpha^*\beta^*} + 2A_{\alpha^*\beta} + A_{\alpha^*} + A_{\beta^*} + A_{\alpha} + A_{\beta}} \times 100 \quad (2)$$

where $A_{(\alpha^*\beta^*)2}$ is total peak areas for the tetrameric species; $A_{\alpha^*\beta^*}$ is total peak areas for the dimeric species in which both subunits are in their holo-forms; $A_{\alpha^*\beta}$ is total peak areas for the heme-deficient dimeric species; A_{α^*}, A_{α}, and A_{β} are total peak areas for the holo-α-chain, apo-α-chain, and apo-β-chain, respectively; and $A_{\alpha\mathrm{N}}$ and $A_{\beta\mathrm{N}}$ are total peak areas for the natively folded globin chains (charge states +7 through +9, vide supra). The results of these computations are presented in Figures 4 and 5. The abundance of ionic

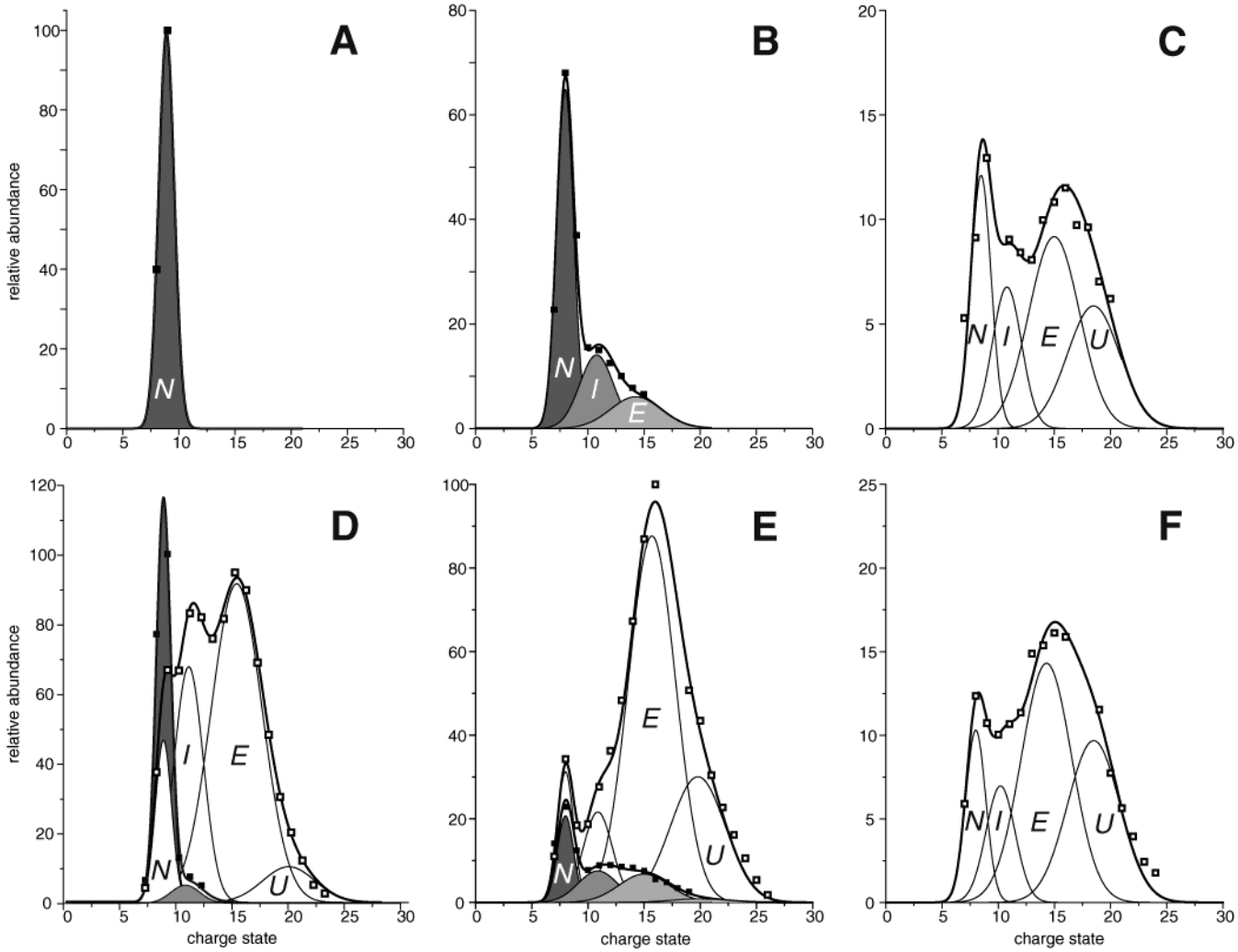

FIGURE 3: Charge-state deconvolution of ionic signal of α- (B, E) and β- (C, F) chains as compared with horse heart myoglobin (A, D) at pH 8 (top row) and pH 4 (bottom row). Closed squares and shaded areas represent holo species; open squares and unshaded areas represent apo species. Two data points were removed from distributions in panels E and F due to significant overlaps of ion peaks corresponding to α- and β-chains at these charge states.

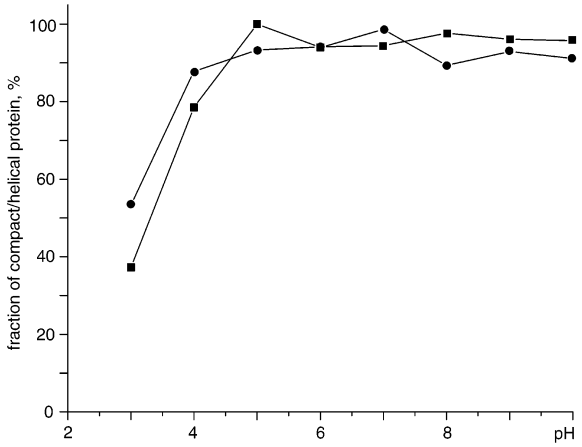

FIGURE 4: Fraction of compactly folded protein as a function of pH, calculated from mass spectral data (■) and far-UV CD data at 222 nm (●).

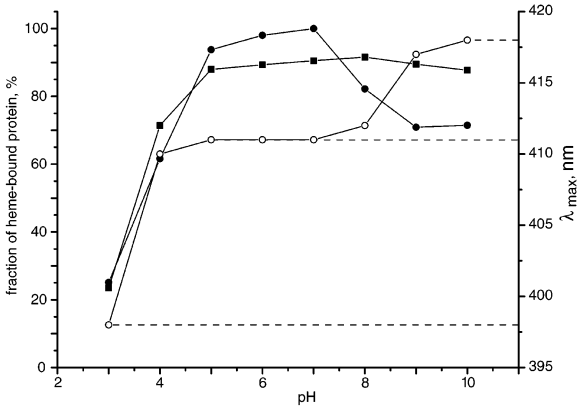

FIGURE 5: Fraction of holo-protein as a function of pH as calculated from mass spectral data (■) and CD data in the Soret region (●). Shift of the CD Soret band (λ_{max}) is shown as a function of pH (○).

species corresponding to compact (highly structured) proteins remains fairly constant within the pH range 5−10 and decreases dramatically at pH < 4 (Figure 4). The percentage of protein with bound heme (holo-protein) shows a very similar trend, as it remains fairly constant within the pH range 5−10 but falls off sharply at pH < 5 (Figure 5).

Circular Dichroism. The far-UV and near-UV/vis CD spectra of hemoglobin are shown in Figures 6 and 7, respectively. The far-UV CD spectra show that hemoglobin has a primarily α-helical structure based on the overall appearance of the spectrum and the negative ellipticity measured at 222 nm. In the pH range 5−10, there is not much

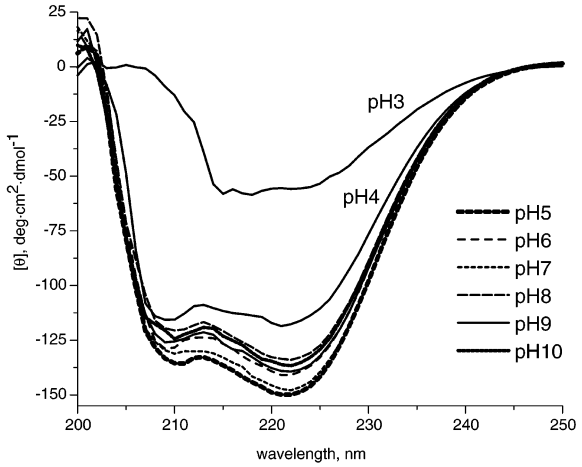

FIGURE 6: Far-UV/vis CD spectra of 10 μM bovine Hb solutions acquired in the pH range of 3−10.

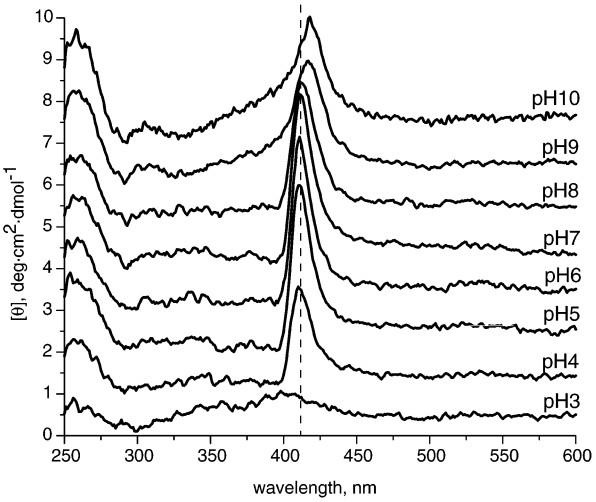

FIGURE 7: Near-UV CD spectra of 10 μM bovine Hb solutions acquired in the pH range of 3−10. Each successive spectrum (beginning with pH 4) has been shifted upward by one unit for clear visualization.

change in the CD spectrum, but further acidification of the protein solution (pH 4 and below) results in significant reduction of the protein helical content and adoption of a more disordered structure.

The molar ellipticity at the Soret band (400−430 nm region) is highest at pH 7. It decreases gradually as the solution pH is decreased from neutral pH to pH 5, followed by a dramatic intensity loss accompanied by a noticeable blue shift at pH 4 and below (from 419 to 398 nm). Some intensity loss is also evident in the CD spectra at elevated pH (above 8) and is accompanied by a red-shift. Summaries of the results of CD measurements in the far-UV region and at the Soret band are presented in Figures 4 and 5.

DISCUSSION

Hb Species in Aqueous Solution. Various Hb forms (tetramers, dimers, and monomeric chains) coexist in aqueous solutions under dynamic equilibrium (*11*), although the crowded cytosolic environment of an erythrocyte usually drives the equilibrium toward the functional tetrameric state $(\alpha^*\beta^*)_2$. While the knowledge of the exact mechanism(s) by which fully functional Hb tetramers are assembled is still lacking, several possible scenarios have been proposed (*16*). These include assembly pathways proceeding through an $\alpha^*\beta^*$-dimer, a heme-deficient dimer (i.e., a heme−globin pair, also termed semi-Hb), or an apo-dimer ($\alpha\beta$). The McDonald group has recently presented strong evidence that in vitro assembly most likely proceeds through the formation of an obligatory $\alpha^*\beta$-intermediate (*16*). The in vivo assembly may proceed through a similar mechanism (with inclusion of globin chaperonins to prevent aggregation at high protein concentration) (*37*, *38*). A goal of the present work was to obtain a more detailed mechanistic insight on the in vitro assembly pathway by monitoring the assembly/dissociation equilibria by ESI MS.

A mass spectrum of the Hb aqueous solution acquired at neutral pH highlights the heterogeneous character of this system (Figure 1). At the concentration used in these experiments, 10 μM, the majority of the hemoglobin molecules is assumed to stay mostly in the tetrameric form, as the tetramer−dimer solution dissociation constant is on the order of 2 μM (*12*, *13*).

The fact that all observed Hb oligomers in Figure 1 contain only even numbers of subunits (no globin trimers are present in the spectra) emphasizes the structural importance of the dimeric species in hemoglobin assembly. The presence of a heme-deficient dimeric species in the mass spectrum alongside the intact dimer $\alpha^*\beta^*$ is significant, as it has been suggested to be an important player in the assembly process (*16*). We note that neither putative apo-dimer $\alpha\beta$ nor heme-deficient tetramers are present in the spectrum. Furthermore, the absence of α- and β^*-monomers from the mass spectrum indicates that the heme-deficient dimer is formed through binding of the apo-β-chain to the holo-α-chain (i.e., $\alpha^* + \beta \rightleftharpoons \alpha^*\beta$), consistent with a hypothesis recently put forward by McDonald and Vasudevan (*17*).

Changes in the position of the equilibrium are evident in the visual differences between the mass spectra (Figure 2) as the solution pH is varied. The spectra are dominated by tetrameric and dimeric species at a pH above 4, consistent with earlier reports that bovine Hb is stable down to pH 4.1 for at least 24 h (*35*). No signal corresponding to an apo-α-chain could be detected within this pH range, highlighting the strength of the heme−globin interaction. Importantly, the onset of heme dissociation from the α-chain (pH 4) coincides with a significant shift in the oligomers/monomers equilibrium, indicating an important role played by α^* in the dimer assembly process (Figure 8).

The total fraction of heme-bound protein (estimated based on the relative intensities of all apo- and holo-protein ions in ESI spectra, eq 2) follows the same trend as the $\alpha^*/(\alpha + \alpha^*)$ (Figure 5). This heme dissociation curve was also compared with the evolution of the Soret band in the pH range 3−10. The absorption Soret band (410−430 nm) arises because of the coupling of the $\pi \rightarrow \pi^*$ transitions of the heme group and neighboring aromatic residues (*39*). In CD spectra, the intensity of the Soret band is governed by the asymmetry of the protein environment (*40*) and is often used as a reporter of structural changes within the heme-binding pocket and indeed the heme dissociation from myoglobin and hemoglobin in solution (*40*). Diminished intensity of the Soret band is usually attributed to disruption of the heme-protein binding (*41*). We note that the evolution of a Soret CD signal is in good agreement with the fraction of heme-bound Hb chains calculated based on the ESI MS data at

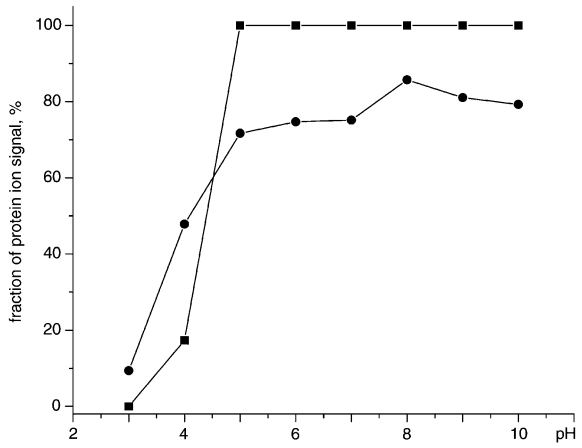

FIGURE 8: Fraction of heme-bound α-globins, α*/(α + α*) (■), and oligomeric Hb species (●) as a function of pH in ESI mass spectra.

pH 7 and below. Both curves have a plateau in the pH range 5−7, indicating a high percentage of heme-bound protein. The onset of heme dissociation is at pH 4, followed by almost a complete disappearance of the signal corresponding to the heme-bound globin chains in both near-UV CD and ESI spectra at a lower pH. The two curves exhibit markedly different behavior at pH 8 and higher; however, the Soret signal in the above-the-neutral pH region cannot be used as a reliable indicator of protein−heme binding. Deprotonation of some noncoordinating aromatic residues in the heme binding pocket are known to result in intensity loss, as well as to a noticeable red-shift of the Soret absorption band in heme−proteins (*42*). Therefore, the observed behavior of the Soret band in the CD spectra of Hb at pH 8 and above cannot be attributed to the heme−globin dissociation.

Flexibility of Globin Chains and Hb Dimer Formation. A unique feature of ESI MS is its ability to provide not only compositional but also conformational characteristics of proteins in solution. Charge-state distributions of protein ions can be used to monitor changes in the protein tertiary structure, as the partially unstructured (less compact) states accumulate a greater number of charges during the ESI process (*43*). This feature of ESI MS has been used in the past to monitor protein conformational changes induced by ligand binding, chaotropic agents, etc. (*23*). It has been recently demonstrated that multiple protein conformers coexisting in solution under equilibrium can be detected and characterized simultaneously based on the protein ion charge-state distributions in the ESI spectra (*36*). Careful analysis of the charge-state distributions of protein ions in Hb spectra reveals that the apo-β-chains are mostly highly charged, possessing a broad charge-state distribution, and the holo-α-chains show significantly lower charge density and narrower charge-state distribution (Figure 1). This suggests that the β-chain exhibits significantly higher flexibility in solution as compared to the α-chain.

To characterize the globin chains' flexibility in a semi-quantitative fashion, charge-state distributions of the two globins from the ESI spectra acquired at pH 7 and 4 have been processed using a chemometric approach described elsewhere (*36*) and compared to that of a structurally similar protein, myoglobin. The α- and β-chains are almost equally divergent from myoglobin (roughly 27% sequence homology), although the tertiary structures of all three chains appear to be almost identical. There is, however, much more similarity in the observed dynamic behavior between myoglobin and the α-globin, as opposed to the β-globin. At neutral pH, the α-globin exhibits only slightly higher flexibility as compared to holo-myoglobin, as evidenced by a low-intensity shoulder in its charge-state distribution extending up to the +15 state (compare Figure 3A,B). Deconvolution of this distribution suggests the presence of two low-abundance partially unstructured conformers, whose charge densities are similar to those of the intermediate states of myoglobin I and E (nomenclature by Callender et al.) (*44*). As with myoglobin (*45*), the heme group remains bound to these states of the α-globin, despite a partial loss of structure. It is possible that these states are only transiently sampled by the α-globin, and the refolding rate is too high to allow the heme−globin dissociation to occur. The refolding rate should be significantly decreased under mildly denaturing conditions, leading to partial dissociation of the heme−globin complex at acidic pH (Figure 3E). Acid-induced loss of the heme group leads to stabilization of the partially unstructured states of the α-globin, processes analogous to that observed with myoglobin (Figure 3D). The β-globin, on the other hand, exhibits a highly heterogeneous character even at neutral pH, with the natively folded conformer being a minor fraction (Figure 3C).

Unlike the individual globin chains, Hb oligomers (both dimers and tetramers) always maintain a compact structure in solution (regardless of pH), as evidenced by narrow charge-state distributions and low charge density of the corresponding ions in the ESI spectra. Thus, the α*β*-dimer ions have an average charge of approximately +12, as compared to an average of +8 of its constituents (in their most compact states). Association of two dimers to form a tetramer results in a further decrease of the average charge per Hb subunit (+18 for $(\alpha^*\beta^*)_2$), consistent with the reduction of the solvent-accessible protein area (*46*). It is interesting to note that the charge-state distribution of the heme-deficient dimer α*β is essentially the same as for the holo-dimeric form of Hb, suggesting that the β-globin flexibility is dramatically reduced upon binding to the α*-chain. Although acidification of the protein solution to pH 4 and below leads to dissociation of Hb oligomers to its constituents, no partial unfolding of the remaining oligomeric Hb species is evident in ESI spectra under any conditions. Therefore, only separate globins may contribute to any loss of tertiary structure. Figure 4 represents a fraction of compact (folded) protein as a function of solution pH, estimated based on the appearance of the ionic charge-state distributions using eq 1. In calculating the percentage of natively folded protein, the dimers, tetramers, and monomers with +7, +8, and +9 charge states of α-, α*-, and β-chains were considered to possess natively folded structures (based on the results of the charge-state deconvolution, Figure 3). This acid-induced unfolding curve was then compared to a progressive loss of helical structure, as determined by far-UV CD. Analysis of CD spectra using the CD trough at 222 nm is perhaps the simplest method to derive the fractional value of helical structure (*47*). The CD spectra acquired in the pH range 5−10 show little change in protein helical content (Figures 4 and 6). A noticeable loss of helical structure occurs when the pH is decreased to 4. A further decrease of pH results in

a very significant loss of helical conformation and an accumulation of unstructured proteins, as evidenced by both the reduction of θ_{222} and the shift of both minima in the CD spectrum (Figure 6). These spectra were used to calculate the evolution of Hb total helical content as a function of pH (Figure 4). Since β-strands are not present in Hb, the α-helix to random coil transition can be used as a quantitative gauge of protein unfolding. This acid-induced unfolding curve is in good agreement with the ESI MS data, as the loss of helical content by Hb (as measured by far-UV CD) appears to be correlated with the loss of Hb compactness (as deduced from the ESI MS charge-state distributions), Figure 4. Both techniques indicate that Hb remains highly structured in the pH range 5−10. The onset of Hb unfolding is at pH 4 (mostly because of the emergence of partially unstructured α-globins), followed by a rapid loss of protein structure at a more acidic pH. It is at this pH that traces of apo-dimers appear in the ESI spectrum (with no signs of either α*β* or α*β), apparently resulting from indiscriminate binding of the apo-forms of α- and β-globins (Figure 2, top trace). It therefore appears that both the native structure and the presence of the heme group in the α-globin are essential for efficient formation of Hb dimers and tetramers. ESI mass spectra of the separated apo-forms of both α- and β-globins (unpublished results from this group) show that both chains in their heme-free forms have a highly flexible structure. Isolated and heme-reconstituted α-chains are monomeric and give rise to a charge-state distribution very similar to that of monomeric α-chains in the ESI spectrum of Hb (as shown in Figures 1 and 3). On the other hand, isolated β-chains mixed with a (molar) excess of heme do show an ability to form tetramers, as well as dimers (β*β* and β*β), although the most abundant species are loosely structured monomeric species (both β and β*). Interestingly, formation of a homo-tetrameric hemoglobin molecule (*Hb H*) is a well-documented clinical consequence of significant overexpression of β-globin in α-thalassemic disorder (*48*, *49*). Such ability of flexible β-globins to undergo ordered oligomerization (as opposed to aggregation) also highlights the extreme importance of chain dynamics and intrinsic disorder for the protein assembly process.

Implications for the Mechanism of Hb Assembly/Dissociation. The analysis of Hb dissociation/assembly equilibria presented above suggests that the in vitro assembly of the functional state of the protein proceeds via the following steps: (i) binding of a natively folded holo-α-globin and a partially unfolded apo-β-globin to form a highly structured heme-deficient dimer, $\alpha^*_N + \beta_U \rightarrow (\alpha^*\beta)_N$; (ii) heme acquisition by a heme-deficient dimer to form a holo-dimer, α*β + heme → α*β*; and (iii) association of two holo-dimers to form tetrameric Hb, $2\alpha^*\beta^* \rightarrow (\alpha^*\beta^*)_2$.

Spirin et al. have demonstrated that α-globin acquires a significant proportion of its native fold and heme-binding capacity cotranslationally (*50*), prior to any interactions with the β-globin. It now seems likely that the latter one emerges from the ribosome in a mostly unstructured, heme binding-incompetent form. However, the binding of such a disordered polypeptide chain (β_U) to a folded α*-chain apparently locks the β-globin in a compact, native-like fold, thus making it competent for a robust heme acquisition. Importantly, these heme-deficient dimers cannot produce higher oligomers (as no heme-deficient tetramers were observed in any of the ESI spectra), thus emphasizing the structural importance of the heme group for the dimer−dimer interface. In fact, the results of this work produce solid evidence that the heme group is vital to the very existence of the $\alpha_1\beta_2$ (but not $\alpha_1\beta_1$) interface. This is not surprising, since even the highly structured apo-β-globin is likely to lack a stable F-helix (by analogy with the native state of apo-myoglobin) (*51*), an element that is crucial for formation of the dimer−dimer interface.

A significant asymmetry exhibited by the two globins in the assembly process highlights the structural and functional importance of disordered protein states. It seems plausible that the rigid α*-chains serve as templates for dimer formation, to which the highly dynamic β-globins can easily adapt. Structural elements that form the $\alpha_1\beta_1$-interface are B-, G-, and H-helices and GH corners of both globins. Significant reduction of plasticity in these segments of the β-globin (following the α*β-dimer formation) apparently makes it competent for heme acquisition (by inducing a stable requisite tertiary structure of the β-globin).

Interestingly, earlier work by Yamaguchi and Adachi suggested that the isolated β-globins form homo-dimers much more readily as compared to the isolated α-globins (*52*). It has also been shown that when unstable β-chain variants are incorporated into dimers with normal α-chains, the dissociation rate to monomers is greater for normal α*β*-dimers than for the dimers containing the unstable β-chain variants (*53*). Combined with the results presented in our work, this suggests that the role of flexible building blocks in the assembly process may actually outweigh the importance of having a correct structural template that directs the binding.

The intimate relationship between protein flexibility and binding has been shown to exist in many cases, as numerous proteins either lack intrinsic globular structure or contain long disordered segments under physiological conditions (*54*). Such structural disorder may be relieved upon binding of the protein to its target molecule. Unstructured protein molecules are believed to have greater capture radii (resulting in significantly enhanced binding kinetics), a feature that is invoked in a recently introduced "fly-casting" model of macromolecular binding (*55*). It is also recognized that the intrinsic lack of structure can confer to a protein the ability to precisely control the binding process (*56*). What makes the apparent intrinsic disorder of the β-globin so surprising is its high sequence homology, near-identical structure, and common origin with the α-globin (*57*), which needs to be tightly folded and contain a heme group for the binding to occur. It is likely that such asymmetry has been developed under the evolutionary pressure to minimize globin aggregation in a crowded cytosolic environment of erythrocytes. The dramatic increase of oxygen demand in higher vertebrates resulted in significant elevation of Hb levels in vascular circulation (*58*, *59*). Simple rheological considerations (*60*) suggest that higher oxygen demands are optimally met by relatively low molecular weight Hb molecules at high concentration (i.e., tetrameric vertebrate as opposed to giant extracellular nonvertebrate hemoglobins) (*61*, *62*). Compartmentalization of such relatively low molecular weight hemoglobins inside erythrocytes minimizes their loss through excretory filters and reduces the solute load on plasma (*58*). Typical Hb concentration inside a mammalian erythrocyte is on the order of 5 mM (*63*), a far higher number as compared to that of a typical erythrocyte-containing inver-

tebrate (*59*). The efficiency of oxygen delivery from lungs to tissue had been further enhanced by highly cooperative ligand binding, as a result of the emergence of two separate Hb chains about 450 million years ago (*49*). However, the presence of two different globin chains (expressed by different chromosomes in mammals) at very high concentration are potentially disastrous, as they may provoke misfolding and aggregation. The asymmetry of globin interaction reported in this work may provide a vital safeguard, which (in addition to recently reported α-globin chaperonins) (*37*, *38*) may inhibit random oligomerization, thus directing the assembly process alongside a correct pathway.

The present work also highlights the utility of ESI MS for studies of both structural and dynamic aspects of protein interaction in highly heterogeneous systems. While most other techniques provide structural data averaged across the entire protein population or biased toward the most stable state(s), mass spectrometry is capable of monitoring both composition and conformation of protein complexes in a species-specific fashion. This may provide a key to understanding mechanisms of such diverse processes as macromolecular assembly and recognition.

APPENDIX

Because of the fragile nature of noncovalent protein complexes, ESI interface conditions typically need to be as gentle as possible to maintain the intact complexes throughout the desorption process (*20*). At the same time, sufficient energy is needed to reduce the residual solvation of protein ions to ensure sensitive detection and confident species assignment. To find optimal conditions for the ESI mass spectral measurements, the influence of the ESI source conditions on the appearance of the Hb spectra was investigated. A selection of these spectra have been included in the Supporting Information. Among several possible noncovalent complex ion dissociation processes, particular attention has been paid to two groups: (i) dissociation of a heme group from globin monomers and oligomers and (ii) dissociation of oligomers to globin monomers.

In our assessment of the dissociation of multiply charged heme−globin complexes in the gas phase, we assumed that the heme group must bear a positive charge, as this is more enthalpically favorable (as compared to the separation of neutral or negatively charged heme group from the positively charged globin). The validity of this assumption is further corroborated by well-documented behavior of a similar heme-containing protein myoglobin in the gas phase (*64*). Since porphyrins have extremely low solubility in aqueous solutions, the heme ionic signal should be attributed to the dissociation of noncovalent heme−globin complexes in the gas phase and can be used as a reporter of such processes. Indeed, progressive elevation of an orifice potential and/or desolvation temperature above those used to acquire the spectrum shown in Figure 1 lead to the appearance and monotonic increase of the signal corresponding to a singly charged heme group with a mass of 616 Da (Supporting Information, Figures 1−3). Importantly, this ion is absent from the spectrum shown in Figure 1, suggesting that the source conditions used in this work do not cause noticeable dissociation of noncovalent heme−globin complexes in the gas phase.

Another important issue that needs to be addressed is a possibility of monomeric globin ions' (both apo- and holo-) formation in the gas phase as a result of the dissociation of oligomeric ions (dimers and tetramers). Gas-phase dissociation of globin oligomers ions has been thoroughly studied by Heck and Versluis (*29*) and Karas and Schmidt (*65*). Karas and Schmidt observed the asymmetric dissociation of a multiply charged Hb tetramer in the gas phase leading to the formation of a trimer ($\alpha^*_2\beta^*$ or $\alpha^*\beta^*_2$) and a complementary monomeric globin (*29*). A similar gas-phase dissociation pattern was also observed for another noncovalent tetramer protein, transthyretin (*66*). Asymmetric dissociation of Hb tetramers (to form trimers and complementary monomers) is evident at high orifice potentials. Thus, elevation of the orifice potential above 130 V leads to the emergence of the $(\alpha^*_2\beta^*)^{+n}$ and $(\alpha^*\beta^*_2)^{+n}$ and heme-deficient trimers ($n = 10, 11$) ion peaks in the ESI spectra of Hb (Supporting Information Figure 1). These peaks are complementary to the monomeric globin ion carrying +7 or +8 charges, which also become prominent in the spectra under these source conditions. None of the trimer ions is present in the spectrum acquired under mild source conditions, suggesting that the Hb tetramer ions do not dissociate in the gas phase under the conditions used in our work.

Dissociation of heme-containing globin dimers in the gas phase has been considered by Heck and Versluis (*29*), who observed uneven charge distribution between the two monomeric fragments. The average charge state of the β-globin ions detected under the mild ESI source conditions actually exceeds that of the dimer ions, effectively disqualifying the latter ones as a possible source of the β-globin ion formation in the gas phase. The α^* -globin monomers detected under the mild ESI source conditions (charge states +7 through +9) may potentially represent the products of the Hb dimer ion dissociation in the gas phase. However, the complementary β-globin ions (charge states +3 through +5) are not detected in the spectra unless the orifice potential is raised to at least 130 V (Supporting Information Figure 1). This suggests that the dimer-to-monomer dissociation does not occur under the conditions used in the present work.

ACKNOWLEDGMENT

The authors thank Prof. Lila M. Gierasch (University of Massachusetts) for providing access to a CD spectrophotometer and Prof. Stephen J. Eyles (University of Massachusetts) for helpful discussions.

SUPPORTING INFORMATION AVAILABLE

Gas-phase dissociation data for bovine Hb. ESI mass spectra showing the effects of progressive elevation of the orifice potential and desolvation temperature. This material is available free of charge via the Internet at http://pubs.acs.org.

REFERENCES

1. Perutz, M. (1997) *Science is not a quiet life: Unravelling the atomic mechanism of haemoglobin*, World Scientific Publishing Co. Pte. Ltd., Singapore.
2. Brunori, M. (1999) *Trends Biochem. Sci. 24*, 158−161.
3. Ivanova, M., Jasuja, R., Krasnosselskaia, L., Josephs, R., Wang, Z., Ding, M., Horiuchi, K., Adachi, K., and Ferrone, F. A. (2002) *J. Mol. Biol. 314*, 851−861.

4. Schrier, S. L. (1994) *Annu. Rev. Med. 45*, 211−218.
5. Manning, L. R., Jenkins, W. T., Hess, J. R., Vandegriff, K., Winslow, R. M., and Manning, J. M. (1996) *Protein Sci. 5*, 775−781.
6. Squires, J. E. (2002) *Science 295*, 1002−1005.
7. Royer, W. E., Jr., Knapp, J. E., Strand, K., and Heaslet, H. A. (2001) *Trends Biochem. Sci. 26*, 297−304.
8. Baldwin, J., and Chothia, C. (1979) *J. Mol. Biol. 129*, 175−220.
9. Perutz, M. F., Fermi, G., Luisi, B., Shaanan, B., and Liddington, R. C. (1987) *Cold Spring Harbor Symp. Quant. Biol. 52*, 555−565.
10. Riggs, A. (1981) *Methods Enzymol. 76*, 5−29.
11. Manning, J. M., Dumoulin, A., Li, X., and Manning, L. R. (1998) *J. Biol. Chem. 273*, 19359−19362.
12. Li, R., Nagai, Y., and Nagai, M. (2000) *J. Inorg. Biochem. 82*, 93−101.
13. Edelstein, S. J., Rehmar, M. J., Olson, J. S., and Gibson, Q. H. (1970) *J. Biol. Chem. 245*, 4372−4381.
14. Hargrove, M. S., Whitaker, T., Olson, J. S., Vali, R. J., and Mathews, A. J. (1997) *J. Biol. Chem. 272*, 17385−17389.
15. Griffon, N., Baudin, V., Dieryck, W., Dumoulin, A., Pagnier, J., Poyart, C., and Marden, M. (1998) *Protein Sci. 7*, 673−680.
16. Vasudevan, G., and McDonald, M. J. (2002) *Curr. Protein Pept. Sci. 3*, 461−466.
17. Vasudevan, G., and McDonald, M. J. (1997) *J. Biol. Chem. 272*, 517−524.
18. Hernández, H., and Robinson, C. R. (2001) *J. Biol. Chem. 276*, 46685−46688.
19. Loo, J. A. (1997) *Mass Spectrom. Rev. 16*, 1−23.
20. Loo, J. A. (2000) *Int. J. Mass Spectrom. 200*, 175−186.
21. Chowdhury, S. K., Katta, V., and Chait, B. T. (1990) *J. Am. Chem. Soc. 112*, 9012−9013.
22. Loo, J. A., Loo, R. R., Udseth, H. R., Edmonds, C. G., and Smith, R. D. (1991) *Rapid Commun. Mass Spectrom. 5*, 101−105.
23. Kaltashov, I. A., and Eyles, S. J. (2002) *Mass Spectrom. Rev. 21*, 37−71.
24. Li, X., Himanen, J. P., Martin de Llano, J. J., Padovan, J. C., Chait, B. T., and Manning, J. M. (1999) *Biotechnol. Appl. Biochem. 29*, 165−184.
25. Wada, Y. (2002) *J. Chromatogr. B 781*, 291−301.
26. Green, B. N., Bordoli, R. S., Hanin, L. G., Lallier, F. H., Toulmond, A., and Vinogradov, S. N. (1999) *J. Biol. Chem. 274*, 28206−28212.
27. Green, B. N., Gotoh, T., Suzuki, T., Zal, F., Lallier, F. H., Toulmond, A., and Vinogradov, S. N. (2001) *J. Mol. Biol. 309*, 553−560.
28. Lei, Q. P., Cui, X., Kurtz, D. M., Jr., and Amster, I. J. (1998) *Anal. Chem. 70*, 1838−1846.
29. Versluis, C., and Heck, A. J. R. (2001) *Int. J. Mass Spectrom. 210*/*211*, 637−649.
30. Loo, J. A., Loo, R. R. O., and Andrews, P. C. (1993) *Org. Mass. Spectrom. 28*, 1640−1649.
31. Apostol, I. (1999) *Anal. Biochem. 272*, 8−18.
32. Light-Wahl, K. J., Schwartz, B. L., and Smith, R. D. (1994) *J. Am. Chem. Soc. 116*, 5271−5278.
33. Chiancone, E., Gilbert, G. A., Gilbert, L. M., and Kellett, G. L. (1968) *J. Biol. Chem. 243*, 1212−1219.
34. Kebarle, P., and Peschke, M. (2000) *Anal. Chim. Acta 406*, 11−35.
35. Fronticelli, C., and Bucci, E. (1994) *Methods Enzymol. 231*, 150−163.
36. Dobo, A., and Kaltashov, I. A. (2001) *Anal. Chem. 73*, 4763−4773.
37. Luzzatto, L., and Notaro, R. (2002) *Nature 417*, 703−705.
38. Kihm, A. J., Kong, Y., Hong, W., Russell, J. E., Rouda, S., Adachi, K., Simon, M. C., Blobel, G. A., and Weiss, M. J. (2002) *Nature 417*, 758−763.
39. Hsu, M., and Woody, R. W. (1970) *J. Am. Chem. Soc. 93*, 3515−3525.
40. Geraci, G., and Parkhurst, L. J. (1981) *Methods Enzymol. 76*, 262−275.
41. Geraci, G., and Li, T. (1969) *Biochemistry 8*, 1848−1854.
42. Papadopoulos, P. G., Walter, S. A., Li, J., and Baker, G. M. (1991) *Biochemistry 30*, 840−850.
43. Konermann, L., and Douglas, D. J. (1997) *Biochemistry 36*, 12296−12302.
44. Gilmanshin, R., Gulotta, M., Dyer, R. B., and Callender, R. H. (2001) *Biochemistry 40*, 5127−5136.
45. Babu, K. R., and Douglas, D. J. (2000) *Biochemistry 39*, 14702−14710.
46. Mohimen, A., and Kaltashov, I. A., manuscript in preparation.
47. Kelly, S. M., and Price, N. C. (2000) *Curr. Protein Pept. Sci. 1*, 349−384.
48. Chui, D. H., Fucharoen, S., and Chan, V. (2003) *Blood 101*, 791−800.
49. Dickerson, R. E., and Geis, I. (1983) *Hemoglobin: structure, function, evolution, and pathology*, Benjamin/Cummings Pub. Co., Menlo Park, CA.
50. Komar, A. A., Kommer, A., Krasheninnikov, I. A., and Spirin, A. S. (1997) *J. Biol. Chem. 272*, 10646−10651.
51. Eliezer, D., and Wright, P. E. (1996) *J. Mol. Biol. 263*, 531−538.
52. Yamaguchi, T., and Adachi, K. (2002) *Biochem. Biophys. Res. Commun. 290*, 1382−1387.
53. Shaeffer, J. R., McDonald, M. J., Turci, S. M., Dinda, D. M., and Bunn, H. F. (1984) *J. Biol. Chem. 259*, 14544−14547.
54. Dunker, A. K., Brown, C. B., Lawson, J. D., Iakoucheva, L. M., and Obradovic′, Z. (2002) *Biochemistry 41*, 6573−6582.
55. Shoemaker, B. A., Portman, J. J., and Wolynes, P. G. (2000) *Proc. Natl. Acad. Sci. U.S.A. 97*, 8868−8873.
56. Dyson, H. J., and Wright, P. E. (2002) *Curr. Opin. Struct. Biol. 12*, 54−60.
57. Hardison, R. C. (1996) *Proc. Natl. Acad. Sci. U.S.A. 93*, 5675−5679.
58. Glomski, C. A., and Tamburlin, J. (1989) *Histol. Histopathol. 4*, 509−514.
59. Glomski, C. A., and Tamburlin, J. (1990) *Histol. Histopathol. 5*, 513−525.
60. Snyder, G. K. (1976) *Science 195*, 412−413.
61. Terwilliger, N. B. (1998) *J. Exp. Biol. 201*, 1085−1098.
62. Weber, R. E., and Vinogradov, S. N. (2001) *Physiol. Rev. 81*, 569−628.
63. Riggs, A. F. (1998) *J. Exp. Biol. 201*, 1073−1084.
64. Li, Y.-T., Hsieh, Y.-L., Henion, J. D., and Ganem, B. (1993) *J. Am. Soc. Mass Spectrom. 4*, 631−637.
65. Schmidt, A., and Karas, M. (2001) *J. Am. Soc. Mass Spectrom. 12*, 1092−1098.
66. McCammon, M. G., Scott, D. J., Keetch, C. A., Greene, L. H., Purkey, H. E., Petrassi, H. M., Kelly, J. W., and Robinson, C. V. (2002) *Structure 10*, 851−863.

BI034035Y